

High-Energy Electron Scattering and the Charge Distribution of Carbon-12 and Oxygen-16*

HANS F. EHRENBERG,[†] ROBERT HOFSTADTER, ULRICH MEYER-BERKHOUT,[‡] D. G. RAVENHALL,[§] AND STANLEY E. SOBOTKA
Department of Physics and W. W. Hansen Laboratories of Physics, Stanford University, Stanford, California

(Received August 20, 1958)

The scattering of high-energy electrons from C¹², reported previously, has been extended to 420 Mev. The elastic and inelastic scattering from the first excited level at 4.43 Mev has been studied between 33° and 70°. The new data are in good agreement with what one would expect from the earlier measurements on C¹² performed at 187 Mev. Additional measurements of the elastic O¹⁶ scattering cross sections of 240-, 360-, and 420-Mev electrons as functions of the scattering angle furnish information on the size and shape of the O¹⁶ nucleus. Pronounced diffraction minima in the angular distributions were observed for C¹² and O¹⁶. The experimental results are compared with the predictions of a theoretical phase-shift analysis derived for the harmonic-well independent-particle model of the nucleus. Preliminary best fits confirm the shell-model predictions for the charge density distribution of these *p*-shell nuclei. The preliminary analysis of the data shows that the length parameter of the well is 1.66×10^{-13} cm for C¹², and 1.76×10^{-13} cm for O¹⁶, thus indicating a slight variation of the curvature of the harmonic well as the *p* shell is filled in.

I. INTRODUCTION

IN two previous papers by Fregeau and Hofstadter¹ and by Fregeau,² the scattering of 187-Mev electrons from C¹² at angles up to 135° was reported. This work has been extended to electron energies of 420 Mev. In addition, the elastic scattering of 240-, 360-, and 420-Mev electrons from the O¹⁶ nucleus has been investigated in considerable detail. The purpose of the present paper is to present these new experimental results, which were obtained as part of a program to study the charge density distribution of the nuclei of the first *p* shell, i.e., those lying between lithium and oxygen. The analysis, while only preliminary and incomplete, has concentrated on a comparison with theoretical predictions of the nuclear shell model. The 187-Mev experiments on carbon indicated^{3,4} that the assumption of a parabolic potential well for the shell model gives better agreement than either the (infinite) square or linear potentials. Accepting this result, we have examined in rather more detail the first-mentioned model, which we find in remarkably good agreement with the 420-Mev experiments.⁵ Various modifications of this model necessary for comparison with these more extensive experiments are noted. Also included are investigations of two phenomenological charge distribu-

tions used in previous work, which do not give such good agreement with the experiments.

The present work is part of a program to study systematically the nuclei in the 1*p* shell. The two nuclei here examined have characteristics which make them particularly well suited for a detailed investigation. Since the first excited levels lie 4.43 (6.06) Mev above the ground state for C¹² (O¹⁶), it is much easier to resolve the elastic-scattering peak from inelastic scattering events than for most other nuclei. Even a slight lack of resolution could have an appreciable effect on the angular distribution of the elastically scattered electrons especially at those scattering angles where the inelastic scattering is greater than the elastic scattering, i.e., at large angles or in the neighborhood of a diffraction dip in the elastic scattering angular distribution. Although in principle any resolution down to 0.1% can be achieved with our present equipment, high resolution inevitably means low beam currents. The beam current available, however, largely determines the minimum cross section which is still measurable within reasonable efforts. This means that those nuclei are best suited for a detailed investigation whose first excited states are highest. A survey of some other 1*p*-shell nuclei like Li⁶, Be⁹, B¹¹, and N¹⁴, however, is being carried out at present and the results will be published later.

II. APPARATUS AND PROCEDURE

These experiments have been performed with the Stanford linear accelerator as a source of electrons. The scattering apparatus used in this work has already been described in several earlier papers.⁶ The beam was analyzed magnetically so that the energy band was 0.35% wide for the measurements at 420 and 360 Mev and 0.60% at 240 Mev. The electron current was measured by a large Faraday cup placed behind the

* The research reported here was supported in part by the joint program of the Office of Naval Research, the U. S. Atomic Energy Commission, and the U. S. Air Force, Office of Scientific Research.

[†] Now at the University of Bonn, Bonn, Germany.

[‡] Now at the University of Heidelberg, Heidelberg, Germany.

[§] Now at the University of Illinois, Urbana, Illinois.

¹ J. H. Fregeau and R. Hofstadter, *Phys. Rev.* **99**, 1503 (1955).

² J. H. Fregeau, *Phys. Rev.* **104**, 225 (1956).

³ See especially Sec. III B of reference 2.

⁴ A comparison of the results for parabolic and square potentials has also been given by L. J. Tassie, *Australian J. Phys.* **9**, 400 (1956); also *Proc. Phys. Soc. (London)* **69A**, 205 (1956).

⁵ A preliminary account of these results was given at the Stanford Conference on Nuclear Sizes; see D. G. Ravenhall, *Revs. Modern Phys.* **30**, 430 (1958). The numerical values given in that paper are, however, too small.

⁶ E. E. Chambers and R. Hofstadter, *Phys. Rev.* **103**, 1454 (1956).

target and was integrated by an Applied Physics Corporation Model 31 vibrating reed electrometer. Beam currents up to a maximum value of 2.5×10^{10} electrons per pulse (2.5×10^{-7} amp) were used (60 pulses per second), but were always kept low enough to avoid any appreciable loss of counts due to pileup. The energy slit of the 36-in. double-focusing magnetic spectrometer was set to 0.35% for most of the measurements which corresponds to an over-all resolution of about 0.5% for a point beam spot. At 240 Mev the detector slit was set at 0.60%, thus limiting the over-all resolution to about $\sqrt{2} \times 0.60 = 0.85\%$. The angular aperture was approximately $\pm 0.83^\circ$ in the horizontal scattering plane and $\pm 2.3^\circ$ in the vertical plane. The over-all angular resolution, however, depends not only on the finite acceptance angle of the analyzing magnet but in addition on the size of the beam spot and on the multiple scattering of the electrons in the target. It is estimated that the over-all angular resolution in our experiments was about $\pm 1.2^\circ$. The electrons were detected and counted in the standard manner with a liquid $C_8F_{16}O$ ($n = 1.276$) Čerenkov counter.

Carbon target (graphite) plates of 0.150 in. thickness and occasionally of twice this thickness were used. The absolute value of the C^{12} elastic-scattering cross section at 420 Mev and 40° , as well as the absolute value of the cross section for inelastic scattering from the 4.43-Mev 2^+ level, were determined by comparison of the corresponding yields of scattered electrons with the yield of electrons scattered elastically from free protons in a polyethylene target. The free proton cross section was taken from Rosenbluth's formula and was computed assuming a proton with an exponential charge distribution of rms radius 0.8×10^{-13} cm. In order to derive the cross-section ratios from the measured areas under the elastic and inelastic C^{12} peaks and the free-proton peak, the $1/E$ dispersion correction allowing for the constant relative momentum acceptance of the spectrometer has to be applied. If $Y(E)$ is the yield of scattered electrons as function of the energy setting of the spectrometer, then $\int [Y(E)/E] dE$ integrated over the peak can in good approximation be set equal to $\{(1/E)(dE/di)\}_E \int Y(i) di$, since the peak is rather narrow, where now the yield $Y(i)$ is expressed as function of the current setting i of the spectrometer and where

$$E' = E_0 / [1 + (2E_0/Mc^2) \sin^2(\theta/2)].$$

In addition the bremsstrahlung straggling correction and the Schwinger-Suura radiative correction must be applied for the free-proton as well as to the C^{12} peak, since the low-energy tails of the peak were cut off at unequal values of $\Delta E/E$.

For the measurements on O^{16} , a water target was used. The target was disk-shaped, 2.50 in. in diameter and 0.300 in. thick. Occasionally targets of 0.200 or 0.400 in. thickness were used. The end windows, sealed with O-rings onto the aluminum target frame, consisted

of 0.001-in. Dural foil. For a 0.300-in. thick water target, this means an $Al^{27}:O^{16}$ atomic ratio of about 1:83, which, although small, gives rise to a background from Al-scattering which proved to be not always negligible. The electron-scattering cross sections of O^{16} and Al^{27} are of the same order of magnitude at most of the scattering angles and energies investigated. In order to correct for the undesirable Al background, an identical, but empty, dummy target was bombarded each time after an elastic O^{16} peak was taken under otherwise unchanged conditions. Subtraction of the Al background determined in this way then could be made. Even around the scattering angle at which the O^{16} diffraction dip occurs, the counts originating from Al scattering amounted only to a few percent of the total number of counts. The absolute O^{16} cross sections were measured just as described for C^{12} . The use of a water target offers the advantage of an exactly known proton- O^{16} ratio. In addition a water target has, as compared to a gas target filled with oxygen to a pressure of 2000 psi, the advantage of a 4.6 times higher O^{16} concentration per cubic centimeter, although this could be counteracted by using a gas target chamber of considerable length along the direction of the beam, especially if cooled down to liquid nitrogen temperature. During the numerous runs which were devoted to the measurements on O^{16} , a gas target of conventional design was once also tried. With the target chamber filled with oxygen up to a pressure of 2000 psi, it was found, however, that the width of the elastic O^{16} scattering peak at half maximum was appreciably wider than that observed with the water target under otherwise unchanged conditions, causing a non-negligible loss in energy resolution. It is believed that this broadening can be ascribed to geometrical effects. Both for this reason and those mentioned above, the gas target was abandoned.

Whereas the water target was always held at an angle of 30° with respect to the direction of the incident beam, measured counterclockwise, the carbon target was rotated in such a way that at each scattering angle the normal to the target bisected the scattering angle. Thus, in the case of the C^{12} measurements, a correction was made for the change in effective target thickness with varying scattering angle.

For O^{16} only the elastic scattering was investigated, since the four lowest excited levels lying between 6.06 and 6.12 Mev could not be resolved from each other with our present apparatus. Angular distributions were measured for elastically scattered electrons of 420, 360, and 240 Mev. In the case of C^{12} , the inelastic scattering from the first excited level at 4.43 Mev was studied to some extent in addition to the elastic scattering at 420 Mev. The measurements were performed in the standard manner. Runs from different nights were always normalized to each other by measuring a standard peak. It turned out that the

angular distributions derived from the areas under the peaks agreed very well with those derived from peak heights. The over-all accuracy of the relative cross sections obtained in these experiments is believed to be about $\pm 10\%$ except for the measurements at the very largest momentum transfers where the cross sections are of order of magnitude 10^{-33} cm²/steradian and smaller. Reproducibility often was better and errors due to counting statistics were often smaller, but even so an error of $\pm 10\%$ is given, allowing for drifts in various parts of the experimental equipment, etc. Besides those already mentioned, no corrections were found to be important enough to be applied to the experimental data.

III. THEORY

The assumptions made in the analysis of the present experiments are essentially the same as have been made in all of the earlier work. Both carbon and oxygen have zero spin, so that the use of spherically symmetric charge distributions is rigorously justified. The neglect of any possible energy dependence of these distributions rests on the demonstrations of Schiff and others⁷ that the dispersion contribution to the scattering is inappreciable, and the good agreement obtained at different energies supports this assumption.

Although the dimensionless parameter $\gamma = Ze^2/hc$ is small for these nuclei, the angular regions examined experimentally cover the first diffraction minimum, where the first Born approximation cannot give accurate results, since it predicts zero cross section there. The numerical results have therefore all been obtained by means of a partial-wave analysis, details of which have been given previously.⁸ As will be seen, however, the Born approximation gives quite accurate information about other features of the cross section, and particularly the *position* of the diffraction minimum. It is necessary to allow for nuclear recoil, but it is only a small effect: the maximum value of v/c , v being the velocity of the nucleus in the center-of-mass system, is only 3.4%. The only dynamic effect of recoil on the scattering (as distinct from changes in kinematics) which it is possible to calculate without a relativistic theory of the nucleus is caused by the exchange of *transverse* photons between the electron and the moving nucleus. It is easy to show that for a spin-zero nucleus, this interaction gives zero contribution to the scattering in Born approximation. The inclusion of dynamic recoil effects in a partial-wave calculation of the scattering has been made by Foldy, Ford, Hill, Hill, and Wills.⁹ They use the Breit interaction to describe the exchange of transverse photons, and relate their results to scattering by a spin-zero nucleus by neglecting terms depend-

ing on the nuclear spin. To the extent that this is the same effect as that we mention, their conclusions are in agreement with the observation we make above, since they find that in carbon at 420 Mev the result of including this interaction is to change the radial parameter in the charge distribution by only 0.7%. Because we were not able to include such effects in our phase-shift calculations, the only allowance we have made for a recoil has been in the angular scale, for which we have assumed that the partial-wave analysis describes most accurately the scattering in the center-of-mass system. (The correction is very small, of order one percent.) Our analysis is therefore somewhat inaccurate in the comparison of absolute differential cross sections. The uncertainties involved are only a few percent, however, and are not important compared with the experimental uncertainties in this quantity.

As in the analysis of experiments on other nuclei,¹⁰ the procedure is necessarily that of trial and error. Charge distributions of various functional forms with variable parameters are inserted into the calculation, and by comparison of the resulting differential cross section with experiment the correct values for the parameters can be determined.

Of great interest for these nuclei, which are in a region where the nuclear shell model has had considerable success in predicting level structure, etc., is an examination of the electron scattering cross section in the light of this model.^{2,4,11} If for simplicity it is assumed that the ground states of these nuclei can be adequately described by the lowest shell-model configuration, $(1s)^4(1p)^{2Z-4}$, then energy level structure, etc., involves specification of, firstly, the shape of the common central potential well; secondly, the strength of the spin-orbit coupling; and thirdly the type, shape, and strength of the residual two-nucleon interaction. Comparison with experiment then allows a determination of some of the functions and parameters involved.¹² The relation of these quantities to those of a real nucleus, obtained by using the observed n - p interaction and making a self-consistent field analysis of the Brueckner-Bethe type, is a problem of such complexity that little is known of it at this time. One can imagine that such a calculation would yield an equivalent central potential which would be fairly smooth, resembling more a parabolic (harmonic oscillator) well than a square well. The results of shell-model calculation do in fact seem to favor the former shape of a harmonic well.

Electron scattering provides an independent check on some of the shell-model assumptions; in this simple

¹⁰ Hahn, Ravenhall, and Hofstadter, Phys. Rev. **105**, 1353 (1957).

¹¹ Comparisons with the shell model using a parabolic well have been made by G. Morpurgo, Nuovo cimento **3**, 430 (1956); R. A. Ferrell and W. M. Visscher, Phys. Rev. **104**, 475 (1956); and M. K. Pal and S. Mukherjee, Phys. Rev. **106**, 811 (1957).

¹² See, e.g., D. Kurath, Phys. Rev. **101**, 216 (1956); **106**, 975 (1957).

⁷ L. I. Schiff, Nuovo cimento **5**, 1223 (1957). This paper also lists and discusses the earlier work on this problem.

⁸ Yennie, Ravenhall, and Wilson, Phys. Rev. **95**, 500 (1954).

⁹ Foldy, Ford, Hill, Hill, and Wills (to be published). We thank those authors for a prepublication copy of their work.

case (lowest configuration only) the elastic scattering depends only on the shape of the central well, and not on any of the other features of the model. (This is true to the extent that "dispersion scattering" is neglected.) A program of interest would thus be to start not from assumed charge distribution, but from assumed shell-model well shapes, and to calculate the dependence of electron scattering cross sections on the adjustable parameters inserted in them. In the earlier experiments on carbon at 187 Mev,³ where it was permissible to use the Born approximation to calculate the scattering, this was done for three simple one-parameter well shapes, namely the infinite square well, the infinite parabolic well, and the infinite linear well. Comparison with the experiment clearly favored the harmonic well, with a length parameter $a = 1.64 \times 10^{-13}$ cm.

Because of the computational complexity that would be involved in starting the partial-wave analysis of the scattering from the shell-model potential, we have not carried out a general program of this kind in the analysis of the experiments at the higher energies. We have considered only the infinite parabolic well $V \propto r^2$, where the function which determines the scattering $\rho_{e.m.}$, has the very simple analytic form

$$\rho_{e.m.}(r) = \sum_P \int d^3r_1 \cdots d^3r_A \psi_{g.s.}^*(r_1 \cdots r_A) \times \delta(r - r_p) \psi_{g.s.}(r_1 \cdots r_A) \\ = \rho(0) [1 + \alpha r^2 / a^2] \exp(-r^2 / a^2), \quad (1)$$

where $\alpha \equiv (Z-2)/3$ is proportional to the number of protons in the $1p$ shell.^{2,4,11} Our avoidance of the term "charge distribution" for this quantity, and an understanding of its subscript, are explained by the observation that the protons in the nucleus themselves have a finite charge distribution (presumably close to that measured for free protons). Thus since $\rho_{e.m.}$ describes the distribution in space of the centers of mass of the protons, the charge distribution is^{13,5}

$$\rho(r) = \int d^3r' \rho_{e.m.}(r') \rho_{proton}(|r - r'|). \quad (2)$$

Because the radius of the proton is considerably smaller than that of the nuclei we are considering (0.76×10^{-13} cm compared with $\sim 3 \times 10^{-13}$ cm) the form chosen for ρ_{proton} is not important. For convenience we choose it to be Gaussian, so that the folding integral can be performed analytically, giving us for $\rho(r)$ the same expression as (1), except that in the exponent a^2 is replaced by $a^2 + a_p^2$, where $a_p^2 = \frac{2}{3} \langle r^2 \rangle_{proton}$.

Another effect which must be allowed for in obtaining a charge distribution from even this simple version of the shell model is that the nuclear wave functions given by the model are not translationally invariant,

i.e., because the shell model has a fixed origin (the origin of the central potential) the system described does not have a center of mass which is fixed in space. The effect this has on $\rho(r)$ for the parabolic-well case has been investigated by Schwartz¹⁴ and by Tassie and Barker.¹⁵ The main modification (of order $1/A$) is to insert into the exponent of (1) a factor $(1 - 1/A)$. There are terms of order $1/A^2$, but for carbon and oxygen they are not important, and we have omitted them. This effect acts independently of the finite proton size.

IV. RESULTS

The shapes examined were the parabolic-well shell-model distribution

$$\rho(r) = \rho(0) [1 + \alpha r^2 / a_{e.m.}^2] \exp[-r^2 / a_{charge}^2], \quad (A)$$

where $a_{charge}^2 = (1 - 1/A) a_{e.m.}^2 + a_{proton}^2$; and the two phenomenological shapes

$$\rho(r) = \rho_0 / \{1 + \exp[(r^2 - c^2) / Z^2]\}, \quad (B)$$

and

$$\rho(r) = \rho_0 [1 + r/b + \beta r^2 / b^2] e^{-r/b}. \quad (C)$$

Shape (B) was used in the analysis of the results for gold, and (C) by Fregeau for carbon at 187 Mev.²

The striking feature of the cross sections for both elements is the deep, narrow diffraction minimum. The observed depth is somewhat decreased because of finite experimental resolution. That the cross section should have this behavior is predicted by the Born approximation. The form factor $F(q)$, defined by

$$F(q) = \int d^3r \rho(r) \exp(iq \cdot r),$$

has for shape (A) the simple analytic form

$$F_A(q) = \left[1 - \frac{\alpha}{2(2+3\alpha)} q^2 a_{e.m.}^2 \right] \exp(-\frac{1}{4} q^2 a_{charge}^2),$$

which has one zero. The angular position of this zero turns out to be a surprisingly close guide to the minimum in the cross section, although the actual shape of $d\sigma/d\Omega$ must be obtained by the partial-wave analysis. In each of the shapes examined, the fitting of the angular position of this dip provides an accurate determination of one of the parameters, mainly the parameter which adjusts the radial size. We have confined our attention to two-parameter shapes, and the best value of the other parameter is then selected by comparing the shape of the cross section away from the dip. Mainly because of time limitation we have not made a least-squares analysis. The extent to which alteration of the parameter spoils the fit with experi-

¹⁴ C. Schwartz (private communication). We thank Dr. Schwartz for an informative discussion of this point.

¹⁵ L. J. Tassie and F. C. Barker, Phys. Rev. **111**, 940 (1958). We thank these authors for a prepublication copy of their work.

¹³ Yennie, Lévy, and Ravenhall, Revs. Modern Phys. **29**, 144 (1957).

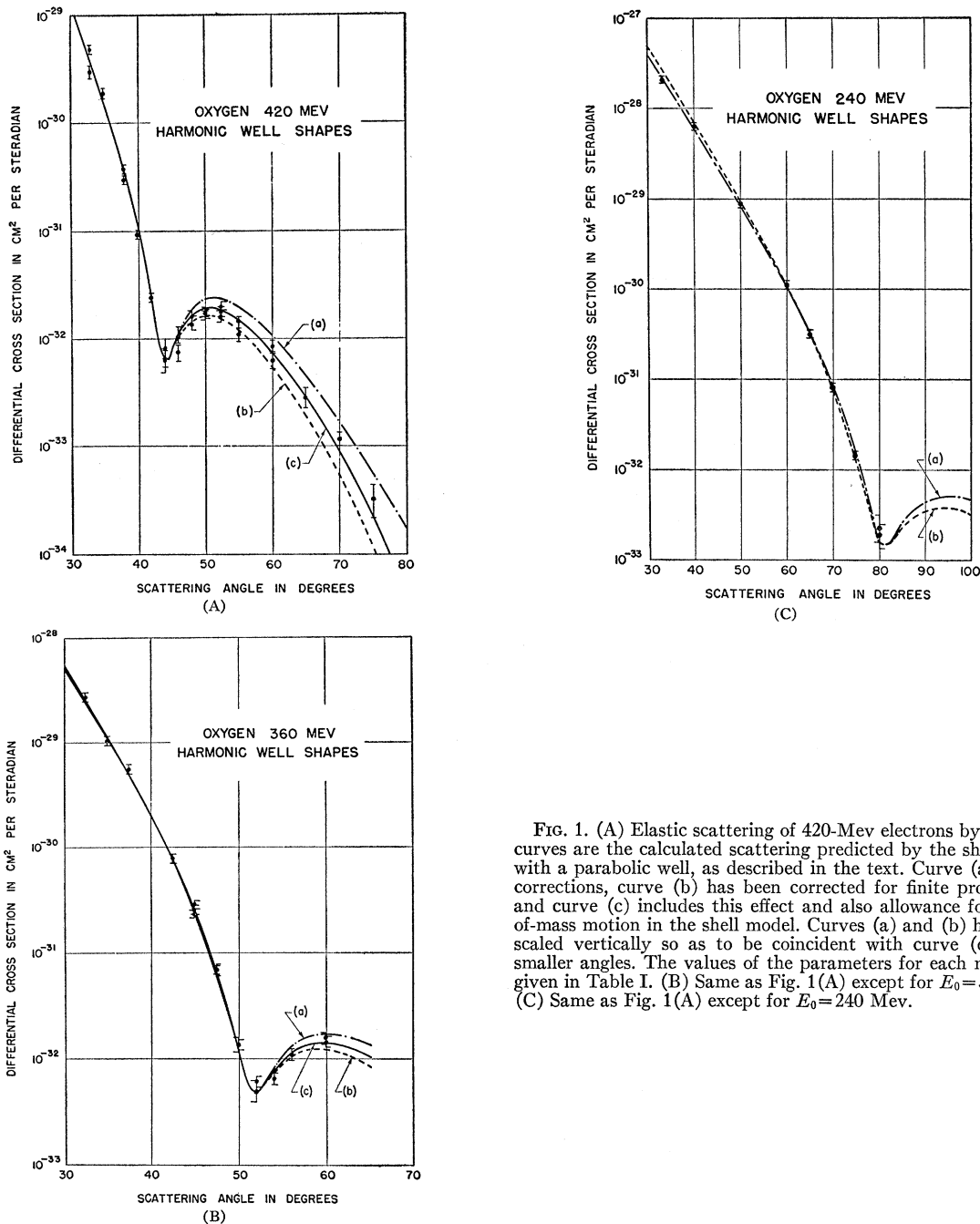


FIG. 1. (A) Elastic scattering of 420-Mev electrons by O^{16} . The curves are the calculated scattering predicted by the shell model with a parabolic well, as described in the text. Curve (a) has no corrections, curve (b) has been corrected for finite proton size, and curve (c) includes this effect and also allowance for center-of-mass motion in the shell model. Curves (a) and (b) have been scaled vertically so as to be coincident with curve (c) at the smaller angles. The values of the parameters for each model are given in Table I. (B) Same as Fig. 1(A) except for $E_0=360$ Mev. (C) Same as Fig. 1(A) except for $E_0=240$ Mev.

ment is determined graphically. Previous experience with other nuclei suggests that with such pronounced diffraction structure a least-squares fit will do little more than confirm the results obtained by graphical fitting.

The comparison of cross sections for the shell-model distribution (A) with the oxygen experiments are shown in Fig. 1. This model contains only one parameter, $a_{c.m.}$, and fixing the position of the diffraction dip determines it. The excellent agreement over the whole

angular range of the 420-Mev experiments [Fig. 1(A)] is a very significant endorsement of this model. The differences between the three versions of the model show up in a pronounced way only beyond the diffraction minimum. Consequently the comparison with the 360- and 240-Mev experiments [Fig. 1(B) and 1(C)], which contain little information in that region, can give not nearly so much information about the charge distribution. The complete agreement at these lower energies is, however, experimental verification that

any energy-dependent contributions to the scattering are inappreciable.

The sensitivity of the agreement with experiment to the radial parameter a is demonstrated in Fig. 2. The three cross sections shown there are all for the complete version of the shell model, including finite proton size and the center-of-mass effect. It is from this comparison that we tentatively propose an error on a of $\pm 0.02 \times 10^{-13}$ cm in the case of O^{16} , although the error on the C^{12} value may be a little larger.

The central potential of the shell model is not actually an infinite well, and it is necessary to find out if the flattening of the well at some large distance, so as to reproduce qualitatively the finite binding, affects the

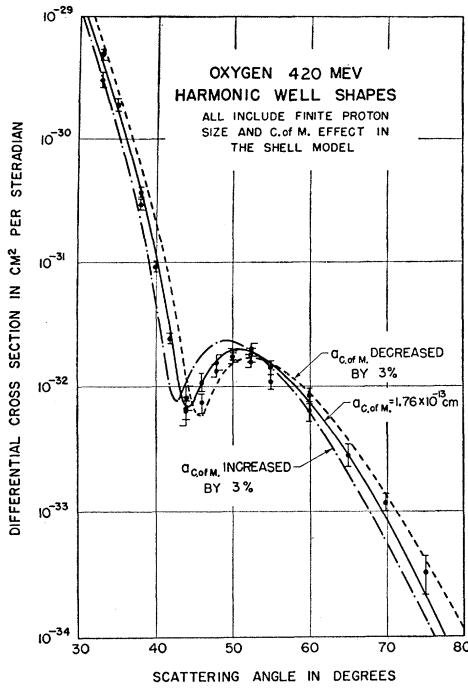


FIG. 2. Elastic scattering of 420-Mev electrons by O^{16} . The curves are all obtained using the complete version of the shell model, corresponding to curve (c) of Fig. 1(A), and show the effect of varying the radial parameter $a_{c.m.}$ by $\pm 0.05 \times 10^{-13}$ cm.

agreement with experiment. To do such a calculation would have involved numerical integration of greater complexity than time allowed, so we investigated this point in an approximate way, by fitting the distribution $\rho_A(r)$ smoothly onto a decreasing exponential charge distribution at a certain radius r_0 . The results for two values of r_0 , corresponding to $1p$ shell binding energies of 10 Mev and 5 Mev, are shown in Fig. 3. In oxygen even the last proton has a binding energy of ~ 12 Mev. It is thus clear from Fig. 3 that the finite binding will have very little effect on the cross section in the angular regions of present interest, although it can change the cross section significantly at larger q values.

The comparison with the carbon experiments is illustrated in Fig. 4. Because the cross section beyond

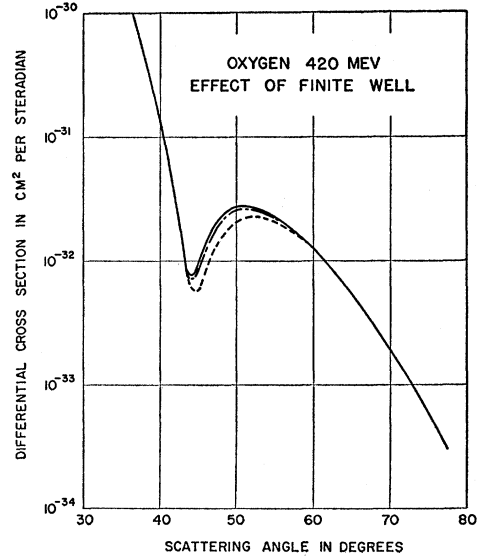


FIG. 3. Theoretical cross sections for O^{16} at 420 Mev. The full curve is curve (c) of Fig. 1(A), and the broken and dashed curves are cross sections obtained by flattening the parabolic well of the shell model at energies 10 Mev and 5 Mev above the $1p$ level, respectively.

the minimum is almost a factor ten smaller than in oxygen, the experimental information is sparser, and the discrimination among the three versions of the

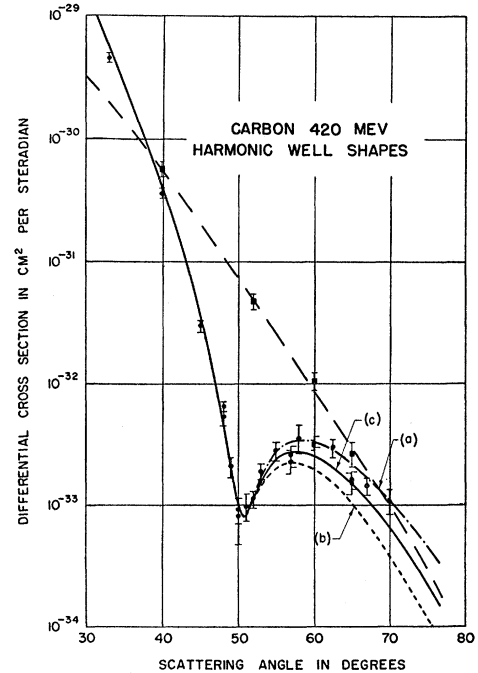


FIG. 4. Elastic and inelastic scattering of 420-Mev electrons by C^{12} . The elastic scattering cross sections are calculated under the same conditions as those for O^{16} , given in the caption to Fig. 1. The inelastic scattering is that arising from excitation of the 4.43-Mev level in C^{12} . The dashed curve is semitheoretical, as is explained in the text. The circles represent the elastic scattering data whereas the squares represent scattering from the 4.4-Mev first excited level.

TABLE I. Values of the parameters obtained from comparison with the 420-Mev experiments of the shell-model charge distribution assuming a parabolic well. The quantities $a_{c.m.}$, a_{charge} , and α occur in the definition below Eq. (A) of Sec. IV. The lengths are in units of 10^{-13} cm. Shape (a) contains no corrections, (b) includes the finite proton size (for a Gaussian proton shape with rms radius 0.76×10^{-13} cm), and (c) contains both this and the effect of center-of-mass motion in the shell model. The parameters α' and a' relate to the charge distribution (1) if regarded as a phenomenological fit to the experiments. The rms radius is obtained from the formula^a $\langle r^2 \rangle^{\frac{1}{2}} = [3(2+5\alpha')/2(2+3\alpha')]^{\frac{1}{2}} a'$.

Nucleus	Shape	$a_{c.m.}$	a_{charge}	α	α'	a'	$\langle (r^2) \rangle^{\frac{1}{2}}_{charge}$
O ¹⁶	(a)	1.76	1.76	2	1.76	2	2.64
	(b)	1.76	1.87	2	1.87	1.34	2.75
	(c)	1.76	1.82	2	1.82	1.60	2.70
C ¹²	(a)	1.65	1.65	$\frac{4}{3}$	1.65	$\frac{4}{3}$	2.42
	(b)	1.66	1.77	$\frac{4}{3}$	1.77	0.94	2.58
	(c)	1.66	1.71	$\frac{4}{3}$	1.71	1.12	2.50

^a Useful formulas concerning form factors of other simple charge distributions, and expressions for rms radii, are given in R. Hofstadter, *Revs. Modern Phys.* **28**, 214 (1956).

shell model is not so clear. There is good agreement with the most complete version (the middle curve in Fig. 4), and this shape gives satisfactory agreement with the 187-Mev experiments of Fregeau.² The numerical values of $a_{c.m.}$ and a_{charge} are presented in Table I, and the charge distributions for O¹⁶ and C¹² are plotted in Fig. 5.

These results can also be regarded as the fit to experiment of a general two-parameter charge distribution of the form (1), with parameters α' and a' to be determined. The values of these parameters are included in Table I. One observes that among the three curves, whose common property is the position of the diffraction minimum, the rms radius varies quite appreciably. This is not surprising, since it is a derived quantity not measured directly in these experiments.

Because of some uncertainties in the effect of recoil which were mentioned in Sec. III, and because experimentally the absolute values of the cross section cannot be obtained so precisely as the relative values from one angle to another, the comparison between theory and experiment on this point is not so fine, although it is

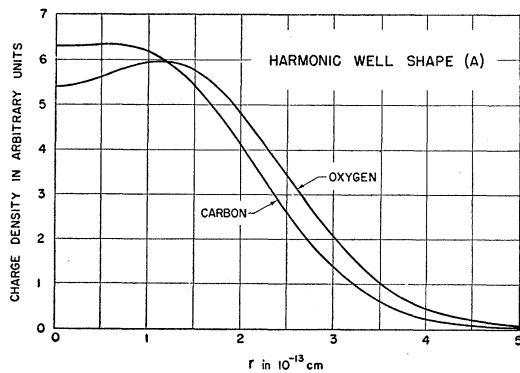


Fig. 5. Charge distributions for O¹⁶ and C¹², as given by the complete version of the shell model with parabolic well, and corresponding curves (c) of Figs. 1 and 4.

still very satisfactory. In Figs. 1(A), (B), and (C), and Fig. 4 the ordinate scale refers to the complete version of the shell model (the other two curves have been shifted vertically). The vertical shift of the whole set of experimental points necessary to obtain an absolute fit was never larger than compatible with the limits of error ascribed to the absolute cross-section measurements. The results of the absolute cross-section measurements, performed as described earlier for both nuclei at one angle at each energy, are listed in Table II.

The experimental results for the inelastic scattering corresponding to the excitation of the 4.43-Mev level in carbon are also plotted in Fig. 4. Since this level is known to be 2+, the transition is $E(2)$. A result of the analysis of the 187-Mev experiments^{3,11} was that the single-particle shell model, with parabolic well, gives good agreement as regards the angular variation of this cross section, but that the absolute magnitude predicted is too low for all modes of coupling. Since a completely collective nuclear model, on the other hand, overestimates the absolute magnitude by a considerable factor,¹⁶ it is reasonable that a small admixture of collective motion can yield the correct value. The dashed curve drawn through the experimental points

TABLE II. Values of the measured absolute cross sections.

Nucleus	Energy Mev	Angle Degrees	$d\sigma/d\Omega$ cm ² /steradian
O ¹⁶	420	40	$(1.0 \pm 0.25) \times 10^{-31}$
	360	55	$(0.9 \pm 0.4) \times 10^{-32}$
	240	60	$(1.1 \pm 0.5) \times 10^{-30}$
C ¹²	420	40	$(3.8 \pm 1.0) \times 10^{-31}$

is therefore semitheoretical, in that its angular variation is that predicted by the shell model, with the same parabolic well as has been used for the elastic scattering. In absolute magnitude, however, it is about 40% lower than one would expect from the 187-Mev results.¹⁷ It is significant that even for these large recoil momenta there is still good agreement with this very simple theory, for the inelastic as well as for the elastic scattering.

The comparison of shapes (B) and (C) with the 420-Mev experiments in oxygen are illustrated in Figs. 6 and 7, respectively. Fixing the position of the diffraction minimum determines a relation between the two parameters in each shape, and a selection of shapes are given. Shape (B) can be made to agree with experiment at all but the largest angles, but shape (C) cannot be made to agree at all. In addition, the absolute cross section for Model (C) is definitely too small. From the plot of charge distributions shown in Fig. 8 we see that in fact shape (C) has about zero central charge density,

¹⁶ See e.g., Ferrell and Visscher, reference 11.

¹⁷ The calculation even with these restrictions is still approximate, in that we have used the Born approximation with suitably modified wave number to calculate the *ratio* of inelastic to elastic scattering, and have then multiplied this ratio by the elastic cross section calculated using the partial-wave analysis.

so that its inability to agree with experiment is perhaps not surprising. This conclusion was earlier drawn by Fregeau, from the analysis of the 187-Mev results on carbon.² Because of the very limited extent of our analysis with arbitrary shapes we cannot draw any general conclusions. It is difficult to see how any shape could give better agreement than (A), the shell-model distribution, but our calculations are not extensive enough to say how far we can deviate from it before there is marked disagreement.

V. CONCLUSION AND DISCUSSION

A comparison has been made between new experiments on C¹² and O¹⁶ at energies up to 420 Mev and

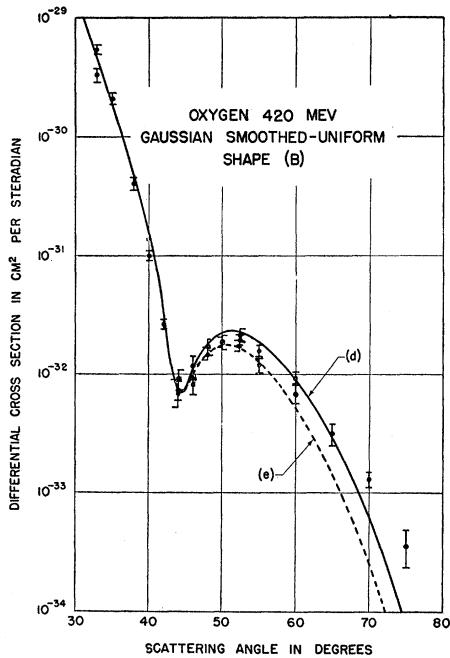


FIG. 6. Elastic scattering by O¹⁶ at 420 Mev. The curves are calculated using shape (B), with parameters (d) $c=2.17$, $Z=1.89$, and (e) $c=2.39$, $Z=1.72$, all in units of 10^{-13} cm. Curve (d) has been scaled vertically so as to coincide with (e) at the smaller angles.

the theoretical predictions of the nuclear shell model, assuming a parabolic central well. After corrections have been made for the finite proton size and the center-of-mass effect, we find for the length parameter $a_{c.m.}$ associated with the parabolic well

$$a_{\text{carbon}} = 1.66 \times 10^{-13} \text{ cm}, \quad a_{\text{oxygen}} = 1.76 \times 10^{-13} \text{ cm}.$$

The error in a_{oxygen} is of order $\pm 0.02 \times 10^{-13}$ cm, and in a_{carbon} somewhat larger. The rms radii of the charge distributions are

$$\langle r^2 \rangle_{\text{carbon}}^{\frac{1}{2}} = 2.50 \times 10^{-13} \text{ cm}, \quad \langle r^2 \rangle_{\text{oxygen}}^{\frac{1}{2}} = 2.70 \times 10^{-13} \text{ cm}.$$

The results obtained without the above corrections are in very good agreement with the earlier value $a_{\text{carbon}} = 1.64 \times 10^{-13}$ cm of Fregeau.² The fact that the rms

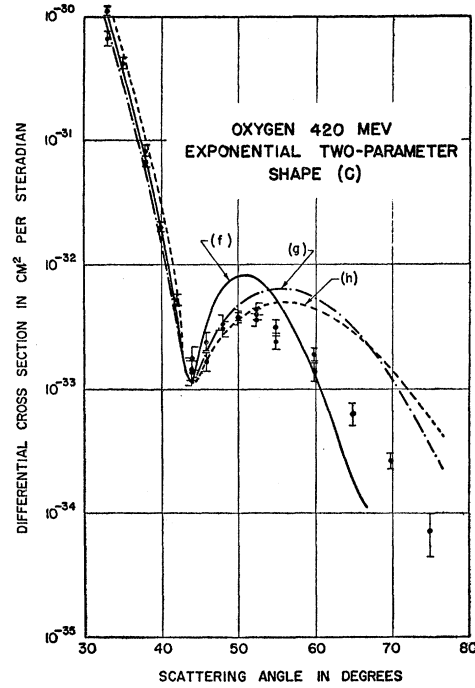


FIG. 7. Elastic scattering by O¹⁶ at 420 Mev. The curves are calculated using shape (C), with parameters (f) $b=0.664$, $\beta=4.7$, (g) $b=0.674$, $\beta=7.5$, and (h) $b=0.645$, $\beta=16.3$. The length parameters b are in 10^{-13} cm. Curves (f) and (g) have been scaled vertically so as to agree with (h) at the diffraction minimum. In order to make a shape fit possible it was necessary to shift the experimental point considerably, as can be noticed from Table II.

radius is somewhat larger than his value is a consequence of the finite proton size: for a folded distribution such as (2),

$$\langle r^2 \rangle_{\text{charge}} = \langle r^2 \rangle_{\text{matter}} + \langle r^2 \rangle_{\text{proton}},$$

and $\langle r^2 \rangle_{\text{matter}}$ is, roughly speaking, fixed by the position of the diffraction minimum. The center-of-mass effect tends to change it in the other direction, but it is not such a large effect.

Another source of information on the well size in the

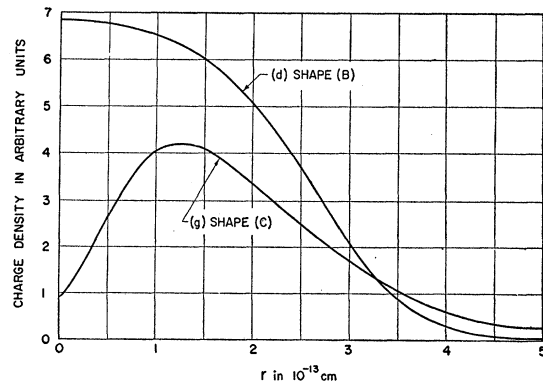


FIG. 8. Charge distributions in O¹⁶, examples of shapes (B) and (C). That labeled (d) corresponds to curve (d) of Fig. 6, and that labeled (g) corresponds to curve (g) of Fig. 7.

shell model is the Coulomb energy of mirror nuclei. A calculation of this quantity for the mirror nuclei $F^{17}-O^{17}$ and $O^{15}-N^{15}$, including exchange effects, was made by Jancovici¹⁸ some time ago. He compared the apparent Coulomb radius $\langle 1/r \rangle^{-1}$ with the rms radius $\langle r^2 \rangle^{\frac{1}{2}}$ and found that in the case of the parabolic well the ratio $\langle 1/r \rangle^{-1}/\langle r^2 \rangle^{\frac{1}{2}}$ was 1.29 and 1.16, respectively, for the two pairs of nuclei. The ratio is, of course, independent of a . If we use for $\langle 1/r \rangle$ the experimental Coulomb energies,¹⁵ and for $\langle r^2 \rangle$ our result for O^{16} , the ratios are experimentally 1.26 and 1.16. The agreement is a very satisfactory check on these two independent measurements of nuclear size.

Experiments are under way on other $1p$ shell nuclei,^{19,20} to investigate in detail the changes occurring as one goes through the shell. The analysis of the elastic scattering will be somewhat more involved, however,

¹⁸ B. A. Jancovici, Phys. Rev. **95**, 389 (1954).

¹⁹ G. R. Bureson and R. Hofstadter, Phys. Rev. **112**, 1282 (1958).

²⁰ U. Meyer-Berkhout (to be published).

since because of the looser binding we may expect nuclei like Li to have more prominent exponential tails to their charge distributions.

ACKNOWLEDGMENTS

We wish to express our thanks to the members of the operating crew of the Stanford linear accelerator for operation of the machine. The phase-shift analyses used in this work were performed by the computer Univac of the California Radiation Laboratory at Livermore. We thank the authorities of this laboratory, particularly Dr. S. Fernbach, for the use of this computer, and Mrs. Mary G. Shepherd and Mr. Charles Emmert for their help in its operation. One of the authors (H.F.E.) is grateful to the "Deutsche Forschungsgemeinschaft" for the grant of a stipend which permitted him to stay at Stanford for one year. Another of us (U.M.-B.) would like to express his thanks to the same organization for financial support during the time this work was performed.

High-Sensitivity Mass Spectrometric Measurement of Stable Helium and Argon Isotopes Produced by High-Energy Protons in Iron*

OLIVER A. SCHAEFFER AND JOSEF ZÄHRINGER†

Chemistry Department, Brookhaven National Laboratory, Upton, New York

(Received September 18, 1958)

A high-sensitivity mass spectrometer has been used to measure the helium, argon, and neon produced in iron by 0.16-, 0.43-, and 3.0-Bev protons. The spectrometer has a sensitivity so that 10^{-11} standard cc of helium could be detected above the contamination level. The He^4 cross sections are 120 mb, 450 mb, and 1300 mb at 0.16, 0.43, and 3.0 Bev, respectively, while the He^3/He^4 cross section ratios are, respectively, 0.09, 0.10, and 0.18. At 0.43 Bev, cross sections of 1.0 mb, 3.3 mb, 8 mb, and 4.1 mb were found for the argon isotopes 36, 37, 38, and 39, respectively. The cross section for neon-21 is 0.1 mb at 0.43 Bev. The results are discussed in relation to evaporation theory and the rare gas content of iron meteorites. The He^3 yields are all higher than previously measured tritium values. At 3 Bev the He^3/T ratio is 2.4. It is suggested that in the case of iron in evaporation theory the Coulomb barrier is not as important relatively as previously thought. Alternatively, a large fraction of the He^3 and tritium may be produced during the nuclear cascade which precedes the evaporation from the excited nuclei. The cross sections measured bear directly on the cosmic-ray-produced rare gases in meteorites. From the cross section of directly produced He^3 relative to T, previous measurements of He^3-T exposure ages of iron meteorites must be reduced by a factor of about 3. From the argon isotope cross sections it is seen that 80% of the Ar^{36} in meteorites is the result of β decay of cosmic-ray-produced Cl^{36} and thus $Ar^{36}-Cl^{36}$ should be a reliable method for measuring exposure ages of meteorites.

INTRODUCTION

WHEN high-energy protons strike a target of a medium-weight element, it has been found that many nuclides are formed below the target mass number. These reactions are being studied extensively at present in many laboratories in the hopes of obtaining

a better understanding of nuclear structure and of nuclear reactions. The general model¹ of the interaction of a high-energy proton is that the proton, during its passage through the nucleus, knocks out several neutrons and protons leaving behind a residual nucleus more or less excited. The excited nucleus then evaporates neutrons, protons, deuterons, tritons, He^3 's, α particles, and possibly other light nuclei, or the excited

* Research performed under the aegis of the U. S. Atomic Energy Commission.

† Assisted by the Deutsche Forschungsgemeinschaft. Present address: Max Planck Institut für Kernphysik, Heidelberg, Germany.

¹ G. Rudstam, *Spallation of Medium Weight Elements* (Uppsala College Press, East Orange, New Jersey, 1956).